A SUPER-OB FOR THE WSR-88D RADAR RADIAL WINDS FOR USE IN THE NCEP OPERATIONAL ASSIMILATION SYSTEM

Jordan C. Alpert[1*], Peter Pickard[2], Yukuan Song[2], Melanie Taylor[2], William B. Facey[1], Michael Istok[2] and David F. Parrish[1].

[1]NOAA/NWS/NCEP, Camp Springs, Maryland 20746

[2]NWS/OST/SEC, Silver Spring, Maryland 20910

1. INTRODUCTION

The spatial and temporal densities of WSR-88D raw radar radial wind represent a rich source of high resolution observations. A characteristic of these observations is the presence of a significant degree of redundant information present in the radar returns. Redundant observations impose a burden on an operational assimilation system since each datum is processed with repetitive interpolations from the analysis grid to its location and back again. This effort is carried out for each datum regardless of the information that can be attributed to it in the overall assimilation. The time and storage expended on mutually redundant data could be better spent on improving other aspects of an assimilation (Purser, et. al., (2000). Therefore, it is desirable to effect whatever data compression the ensemble of fresh observations allow while minimizing any degradation of the information content. The term for a surrogate datum which replaces several partially redundant actual data is a "super observation" or "super-ob".

Super-obs have been applied to operational analysis at the National Center for Environmental Prediction (NCEP) Operational assimilation system for subsets of the WSR-88D radar radial wind observations from the NEXRAD Information Dissemination Service (NIDS). However, the precision and information content of the NIDS radial wind can be improved if data at each radar site is directly utilized at the resolution and precision of the WSR-88D radar to construct the super-ob and then delivered to a central site. We report a new product for the Open RPG software system called the Radar Super-ob which takes the result of radar scans and averages data points within a prescribed time and spatial 3-dimensional volume before transmitting reports to a central collection of base data. The new product will be super-obs of radar radial winds.

*Corresponding author address: Jordan C. Alpert, DOC/NOAA/NWS/NCEP/Environmental Modeling Center, 5200 Auth Road, Rm. 207, Camp Springs, MD 20746; e-mail: jordan.alpert@noaa.gov

2. DESCRIPTION

The full-resolution WSR-88D base radial wind data provides sufficient data amounts for statistically significant averaging. The super-ob product is programmed using the Open Systems RPG (Radar Product Generator) to control all aspects of the calculation at WSR-88D radar sites. The Open RPG is the system which operates between the Open Radar Data Acquisition (RDA) system and more sophisticated display devices, such as the National Weather Service's Advanced Weather Interactive Processing System (AWIPS). The Open RDA collects data from the WSR-88D radar and forwards base data products to the Open RPG. These base data products consist of reflectivity, radial wind, and spectrum width. The Open RPG creates the special purpose products from the base data and forwards them to other systems for display or for further processing. Super-ob is one of the newly enabled, enhanced products under the Open RPG.

Adaptable parameters for super-ob are the Time window, Cell Range Size, Cell Azimuth Size, Maximum Range and Minimum Number of Points. The values of these parameters, which define the super-ob averaging, are shown in Table 1. The default settings indicate that at each elevation angle, a wedge shape volume of 6

Table 1. Adaptable parameters for the Super-ob product.

Parameter	Default	Range
Time Window	60 minutes	[5-90 min]
Cell Range Size	5 km	[1-10 km]
Cell Azimuth Size	6 degrees	[2-12 deg]
Maximum Range	100 km	[60-230km]
Minimum Number of Points required	50 unitless	[20-200]

azimuth degrees by 5 km along a radius, averaged over a time of 60 minutes define each super-ob cell. Each of the super-obs contain no less than 50 points and no cell

would extend past 100 km, as the radar beam width becomes too wide and returns become less certain at larger distances from the radar. These adaptable parameter values are programmed through the Open System RPG (ORPG). The range of possible values will allow for the super-ob product to adjust to different analysis resolution requirements. All the WSR-88D installations will contribute super-ob data to initialize cycling analysis systems, with identical settings through the ORPG. The data transmission precision of the super-ob (mean) radial wind is ±0.01 m/s or 32767 possible levels. This is an improvement over the current transmission of 15 levels of data transmission precision for winds which can span ±100 m/s. The standard deviation of the mean radial wind super-ob is transmitted at 15 levels of precision.

3. RESULTS

A number of tests have been made of the radar system within the Systems Engineering Center at the NOAA/NWS Office of Science and Technology. An example of the Radial wind scalar is shown on a vector plot in Fig 1 where the arrow direction is toward or away from the radar and colors, as well as arrow length, indicate the speed of the return. The Data for this example is from KATX, the Seattle, WA radar from May 28, 2002 at 1800Z and represents a typical return. The

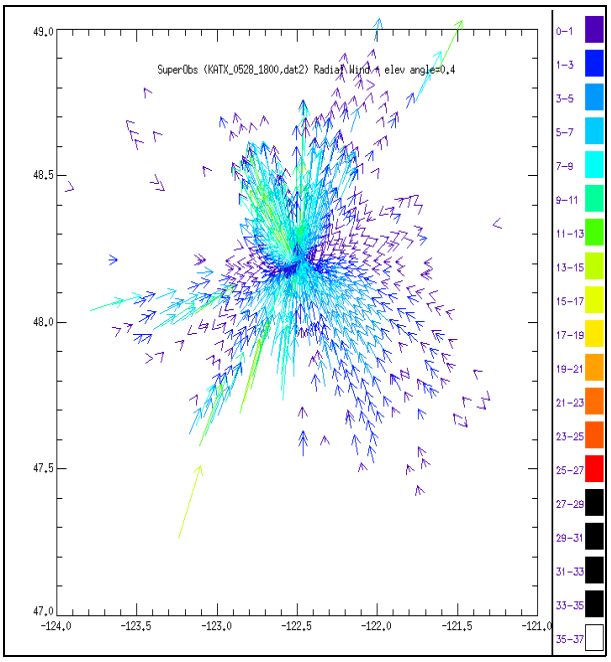

Fig 1. Radar radial (scalar) wind super-obs speed and location from station KATX in Seattle, WA on May 28, 2002. Arrows are toward or away form the radar with the color and arrow length indicating the speed of the return.

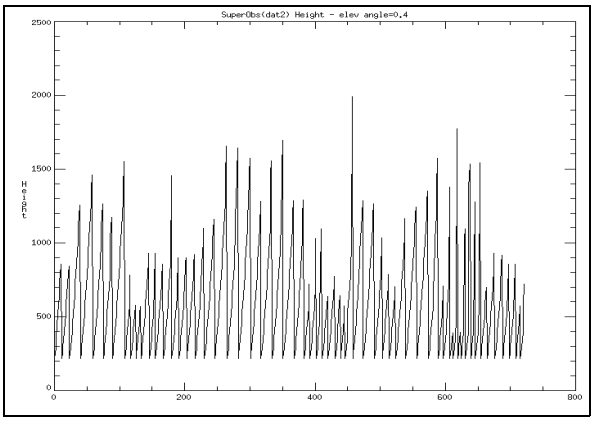

Fig 2. Super-ob height [m] for each observation beginning at 0 azimuth (north) and extending through larger radii and 360 degrees (clockwise) for the same time as in Fig 1.

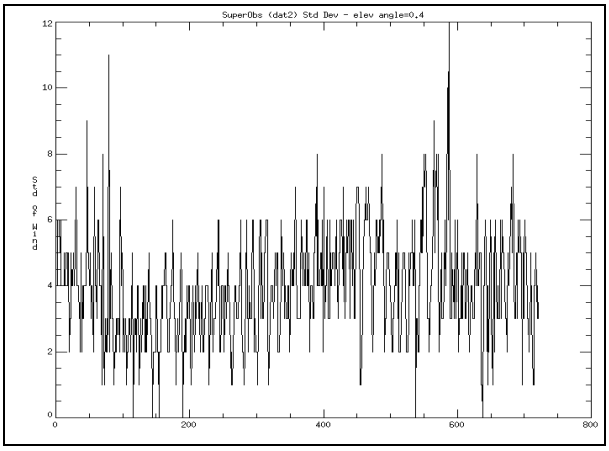

Fig 3. Super-ob radial wind Standard deviation [m/s] for each observation beginning at 0 azimuth (north) and extending through larger radii and 360 degrees (clockwise) for the same time as in Fig 1

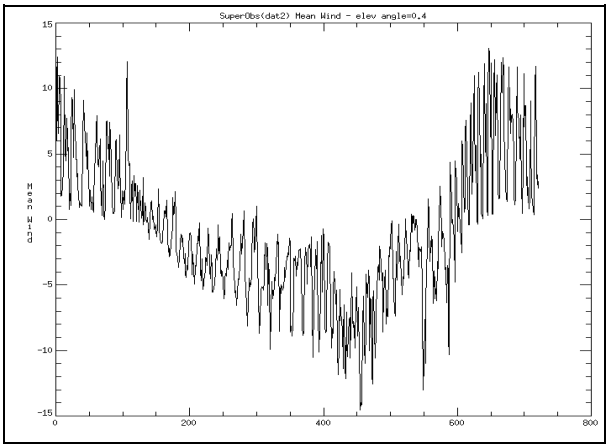

Fig 4. Super-ob radar radial (mean) wind [m/s] for each observation beginning at 0 azimuth (north) and extending through larger radii and 360 degrees (clockwise) for the same time as in Fig 1.

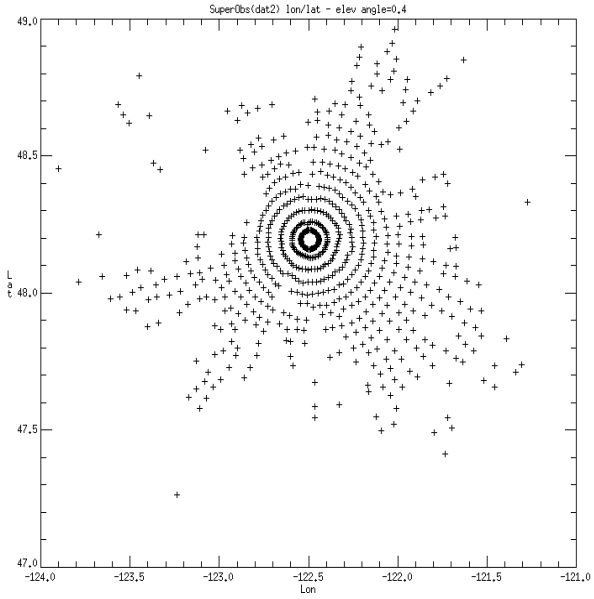

Fig 5. Super-ob radar radial wind location [longitude & latitude] for each observation for the same as in Fig 1.

characteristic pattern of radar radial returns is apparent and there are large areas that do not have returns. At larger distances from the radar the radial wind is seen to increase southwest and northeast of the radar. In a clear air test at station KCRI, the Norman, OK test radar, (not shown) the coverage was more complete. The number of super-ob returns near the radar has not been reduced at this time although there is code to accomplish this and may be done in the future. As the radar beam extends to larger radial distance from the radar, the height of the super-ob increases. In the case of the radial wind shown in Fig 1, at the lowest elevation angle, the height ranges from about 250 m to 2 km. Higher elevation angles have heights that extend from 1 km to throughout the entire troposphere. One way to show the height variation is to plot the super-ob data set according to the first observation which is along 0 degrees north closest to the radar extending out to larger distance from the radar, and then clockwise around in azimuth for the remaining returns in the report, in this case over 700 super-obs. The height in meters is displayed this way in Fig 2. Each point is the result of the super-ob at the next 5 km radius increasing its height as the radial distance increases and then clockwise from north around with increasing azimuth.

Fig 4 shows each super-ob radial wind plotted in this fashion where a sinusoidal pattern of the radial wind results due to the radial wind definition. Each successive super-ob moves out alone the radii with increasing beam height causing a range of super-ob wind magnitudes along each azimuth. The super-ob returns labeled "mean wind" in Fig 4 range from a few m/s near point 200 to 10 m/s near point 650. This range of wind values is from varying height and location of the return and the result of natural variance in the winds in the radar vicinity due to synoptic conditions. However, a number of super-ob wind values in Fig 4 extend beyond the normal range as defined by its neighbors. One can scan this data set and find values outside the range of the super-ob wind and compare with the standard deviation, height and the location of a return in question.

Radial wind speeds at the top of the height range, for each radar beam elevation angle, in Fig 2 (elevation angle = 0.4), sometimes appear less correlated with their neighbors (Fig 4). For example, point 108 at 48.85 at (lat, lon), (48.85, -121.632) have a super-ob wind of 12.1 m/s at a height of 1549 m. Points 458 and 474 at (47.263, -123.238) and (47.579, -123.110) respectively, located on Fig 1, show radial wind magnitudes of -14.12 m/s and -12.58m/s on Fig 4 which is outside the range of common values. The returns for these super-obs are expected to have larger wind magnitudes with increased elevation. The variance for these points is low, 2 m/s, for each point. An example of a high standard deviation return is shown for point 589 at (48.039, -123.789) with a standard deviation of 12 m/s and wind magnitude of -10.33 m/s. The height for point 589 is 1572 m which makes it among the larger distances from the radar and higher height for this radar elevation angle. Fig 3 shows a moderate spike at point 589 in line with the increased height in Fig 2 and the increased negative super-ob wind. In this case, the value is suspect because of the large standard deviation in the radar radial winds making up the super-ob. One may expect a larger standard deviation of radial wind values because of the widening of the radar beam width with increasing distance from the radar as well as with increased wind speeds at higher altitudes. When the radar beam grows wider with increasing distance from the radar, the vertical position of the return can not be determined with precision. The standard deviation, although transmitted as a 4 bit marker (15 levels), can be useful in determining the quality of the returns. The quality control of the super-ob data in the analysis program may also be able to utilize the reflectivity to determine locations of severe convection (and vertical motion) which could cause errors in the radial wind returns. The standard deviation can also be large at points that have less than 1 m/s winds such as points 630, 638, and 639 and 634. In this case these were among the nearly calm values located north and west of the radar (Fig 1).

Fig 5 illustrates the location of each super-ob. The centroid of WSR-88D returns making up each super-ob is calculated and made part of the transmitted header of each super-ob value. If actual returns are weighted toward the longitude and latitude position, then the super-ob location will reflect this. This is the reason the super-ob locations, shown by a "+" in Fig 5 or the tails of the vectors in Fig 1, are not orientated in exact concentric circles. This is also done in time as several scans are averaged to construct the super-ob (Table 1). The time deviation, accounting for the number of raw radar returns differing in each scan are transmitted in the super-ob header.

Close to the radar, the raw return numbers are sufficient to create super-obs under the criterion of Table 1 even though the super-ob area grows smaller. At higher resolution (smaller super-ob area) the near radar super-obs will not have enough returns to satisfy the minimum number of points required to form the super-ob. This criterion may be adjusted so the number of super-obs will be thinned out or the large number of super-obs in close to the radar shown in Fig 5 can be decreased by directly removing super-obs as a function of radial distance from the radar.

4. ANALYSIS AND VERIFICATION

The super-ob examples shown herein are typical of a number of examined preliminary data sets. Fig 6 shows analyzed regular winds at a height of 0.4 km from the NCEP Global Forecast System (GFS) Spectral Statistical Interpolation (SSI) Analysis of May 5, 2002 at 18Z. The wind barbs are displayed over the same domain and time as the super-ob radial wind observations in Fig 1. The operational SSI uses all available remote and conventional observations to create the analysis at a resolution (spectral triangular truncation T170) of less than 1 degree of latitude and longitude. It is plotted at 1 degree in the figure. We can use the SSI analysis as a proxy for observed winds in the radar area as the number of in conventional wind observations in the area depicted around the radar are few. The black cross hair in Fig 6 is located at the Seattle, WA radar location. The regular winds shown in Fig 6 are at a height of 0.4 km which was interpolated vertically by the SSI analysis. The super-ob radial winds located close to the radar are at or near a height of 0.4 km as shown in Fig 2. In viewing the analyzed regular winds, composed of wind components (**u,v**), in Fig 6, one must keep in mind the definition of radial wind:

$$\mathbf{u}_{radial} = \mathbf{u}\cos\theta + \mathbf{v}\sin\theta$$

is a scaler, where θ is the angle between a line from the radar directed at 0 degrees azimuth (north) and the radial

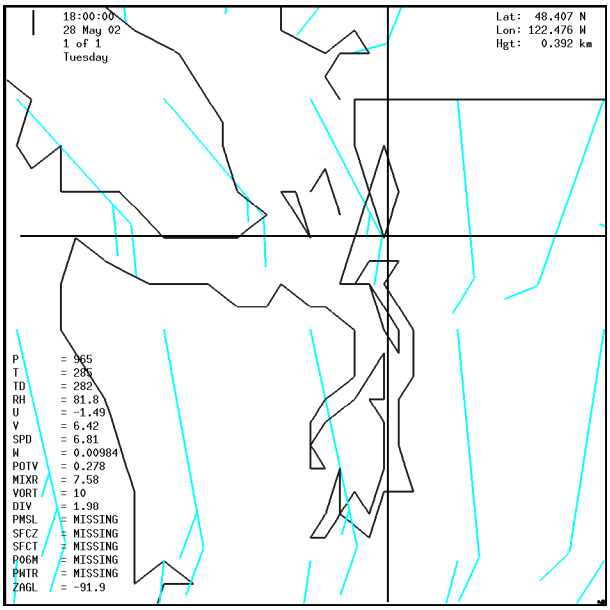

Fig 6. Analyzed regular Wind barbs (blue) at 0.4 km height from the NCEP Global Forecast System Spectral Statistical Interpolation Analysis of May 5, 2002 at 18Z. The black cross hair is at the Seattle, WA radar location.

wind azimuth. There is one direction where the regular wind will be identical to the radial wind and regular winds perpendicular to this will have zero radial wind.

The direction of the regular wind north and west of the radar in Fig 6 is southwest at 15 knots. The radial wind along a line northwest of the radar line up in the same direction. The radial wind speeds in the northeast quadrant vary from 5-15 knots close in as shown by the blue and green wind arrows in Fig 1. To the east of the radar, the wind magnitudes are far less, 0-5 knots. This is because of the radial wind definition and the winds in this region being more southerly and of lower magnitude (Fig 6) so their component in the radial direction will be small. The analyzed winds in the southwest quadrant (Fig 6) tend toward larger magnitudes as do the radial winds shown on Fig 1. Plots of 1 km and 1.5 km regular analyzed winds (not shown) show that winds at higher elevations in this area have increased magnitudes even though the angle of the wind (southerly) and the radial wind are at large angles. The regular winds in the southeast quadrant are SSE with similar magnitudes to the radial wind. That we show consistent magnitudes of the radial wind along the SE - NW direction as the observed winds is a necessary condition for acceptance of the data by the analysis system. The analyzed regular winds in the southeast and northwest quadrants show changes that are reflected in the radial wind pattern as a turning of the regular wind direction from south to

southwesterly. This is an example of the high resolution potential of the radar radial wind data set.

4. SUMMARY AND FUTURE WORK

Implementation of the new super-ob product is scheduled for the fall of 2002. Once the radial wind super-obs are received at NCEP they will be used in the analysis cycling system to become a component, with the other remotely sensed and conventional observations, providing a high resolution wind component. In addition to tests run with and without the presence of the radial winds from the full complement of WSR-88D radars, Purser, et. al., (2000), have shown an objective means of quantifying the information lost by the conversion of many raw data into few super-obs. Refinements about the decisions made on the size of clusters of raw data in space and time can be rationalized using methods of information theory as described in the Purser, et al (2000) approach. A comparison with the NIDS form of the data will be also done. Work continues to extend the super-ob to distances beyond 100 km from the radar. Data and plots of other elevations and radar stations are available at the web site:
http://sgi62.wwb.noaa.gov:8080/SUPEROB.
The raw data for this report is located at:
http://sgi62.wwb.noaa.gov:8080/SUPEROB/read_superob.
The pre-print figures shown in this report are located at:
http://sgi62.wwb.noaa.gov:8080/SUPEROB/AMSFIGURES.

4. REFERENCES

Purser, R. J,, D. Parrish and M. Masutani, 2000: Meteorological observational data compression; an alternative to conventional “super-obbing”, Office Note 430, DOC/NOOA/NWS/NCEP, 5200 Auth Road, Camp Springs, MD 20746-4304,12pp.